Adsorption profile of lead on *Aspergillus versicolor*: A mechanistic probing

Himadri Bairagi [a], Md. Motiar R. Khan [b], Lalitagauri Ray [a], Arun K. Guha [b],*

[a] *Dept. of Food Technology & Biochemical Engineering, Jadavpur University, Kolkata 700032, India*
[b] *Dept. of Biological Chemistry, Indian Association for the Cultivation of Science, Kolkata 700032, India*

ARTICLE INFO

ABSTRACT

The adsorption of lead on *Aspergillus versicolor* biomass (AVB) has been investigated in aqueous solution with special reference to binding mechanism in order to explore the possibilities of the biomass to address environmental pollution. AVB, being the most potent of all the fungal biomasses tested, has been successfully employed for reducing the lead content of the effluents of battery industries to permissible limit ($1.0\,mg\,L^{-1}$) before discharging into waterbodies. The results establish that $1.0\,g$ of the biomass adsorbs $45.0\,mg$ of lead and the adsorption process is found to depend on the pH of the solution with an optimum at pH 5.0. The rate of adsorption of lead by AVB is very fast initially attaining equilibrium within 3 h following pseudo second order rate model. The adsorption process can better be described by Redlich–Peterson isotherm model compared to other ones tested. Scanning electron micrograph demonstrates conspicuous changes in the surface morphology of the biomass as a result of lead adsorption. Zeta potential values, chemical modification of the functional groups and Fourier transform infrared spectroscopy reveal that binding of lead on AVB occurs through complexation as well as electrostatic interaction.

1. Introduction

Lead is a highly toxic metal and its exposure even at low concentration leads to adverse effects on human health particularly in the nervous and reproductive system as well as in kidneys, liver and brain [1,2]. The metal enters into environment as a result of various industrial activities such as electroplating, battery manufacturing, pigment and dye industries, lead smelting and using leaded petroleum engine fuels [3,4]. Because of toxic nature, the concentration of lead in the industrial effluents must be brought down to permissible limit ($1.0\,mg\,L^{-1}$) before discharging into public sewers as per instruction of Environmental Regulatory Authority, India. The available methodologies that are employed for the treatment of lead containing wastewater include precipitation with lime, ultrafiltration, reverse osmosis or ion exchange process [5,6]. However, these methods suffer from limitations like poor cost effectivity, incomplete precipitation, etc. In addition they generate huge amount of toxic metal bearing sludge difficult to dispose of. Thus research on the development of effective and inexpensive technology to treat toxic metal bearing wastewater is very important.

In recent years considerable attention has been focused on adsorption technology to remove metal ions from wastewater from the standpoint of eco-friendly, effective and economic considerations. Of the different adsorbents like saw dust, rice hulls, palm kernel husk, coconut husk, banana and orange peels, modified lignin, de-oiled allspice husk and different agricultural by-products [7,8]; activated carbon, is the best. However, its use is much restricted due to high cost in many countries including India. This leads to search for efficient adsorbents preferably biological materials covering microbial biomass to remove metal ions from wastewater known as biosorption or bioaccumulation [9]. This method has certain advantages over conventional ones, e.g., non generation of toxic sludge, effective in reducing the concentration of metal ions below the permissible limit and the possibility of recovery of the biomaterials by regeneration. Thus it provides an economic means for the treatment of wastewater [7]. The uptake of heavy metals by microbial biomass is a two step process involving initial cell surface binding followed by intracellular accumulation which takes place only in living cells [10]. Adsorption of metal ions on the biomass occurs through electrostatic, physical and chemical interactions with the functional groups present on the cell wall [11–13]. Volesky [14] has recently reviewed the state of art in the field of biosorption of heavy metals. However, only a few reports are available on fungal systems [15,16]. Fungal biomass has certain advantages over bacterial biomass in respect of processing and handling of the biomass. The fungal genera of *Rhizopus* and *Penicillium* [17,18] and the use of raw and pretreated *Aspergillus niger*

* Corresponding author at: Dept. of Biological Chemistry, Indian Association for the Cultivation of Science, 2A & B, Raja S.C. Mullick Road, Jadavpur, Kolkata, West Bengal 700032, India. Tel.: +91 33 2473 4971/5904x502; fax: +91 33 2473 2805.
  E-mail addresses: arunkumarguha@yahoo.com, arunkumarguha@gmail.com, bcakg@mahendra.iacs.res.in, bcakg@iacs.res.in (A.K. Guha).

for the removal of lead, cadmium, copper and nickel have already been reported by other workers [13,19–21]. Several reports including those from our group are also available regarding the use of fungal adsorbents for the removal of metal ions from wastewaters [22–25]. The efficacy of any biosorbent depends on the microenvironment of the targeted toxicant and also on the availability of the material. Thus there is always a need for search of new biosorbents. Further an intimate understanding of the adsorption mechanism is also a prerequisite for improving the efficiency of the process.

The present communication reports the application of *Aspergillus versicolor* biomass for the removal of lead from aqueous environment. In-depth investigations have been carried out to understand the role of associated physicochemical properties involved in the adsorption process of lead from its aqueous medium. Fourier transform infrared spectroscopy (FTIR), energy dispersive X-ray analysis (EDXA) and scanning electron microscopic studies have explored the mechanistic aspects of lead adsorption on *A. versicolor* biomass (AVB) at the molecular level.

2. Materials and methods

2.1. Microorganisms

Rhizopus oryzae (MTCC 262), *A. versicolor* (MTCC 280) and *A. niger* (MTCC 281) were obtained from the Institute of Microbial Technology, Chandigarah, India. *Termitomyces clypeatus* was kindly provided by Dr. S. Sengupta, Indian Institute of Chemical Biology, Kolkata, India. The organisms were maintained on potato dextrose (20% potato extract and 2% dextrose, and 1.5% agar pH5.0) slants by subculturing at regular interval of 30 days.

2.2. Chemicals

All the chemicals and ingredients of microbiological media used in this study were obtained from E. Merck, Germany and Hi Media, India, respectively.

2.3. Preparation and estimation of lead solution

A stock solution of lead (1000 mg L^{-1}) was prepared by dissolving the required amount of Pb(NO$_3$)$_2$ in double distilled water and diluted to get the desired concentration. The concentration of lead in the solution was measured by a flame atomic absorption spectrophotometer (Chemito AA203).

The uptake of lead by the biomass was calculated using the following mass balance equation:

$$q_e = \frac{(C_0 - C_f)V}{1000W}$$

where q_e is the amount of lead uptake by the biomass in mg g^{-1}. C_0 and C_f are the initial and final metal ion concentrations in mg L^{-1} in the solution, respectively. V and W represent the volume of solution (L) and weight of the biomass (g), respectively. The concentrations of sodium, potassium, calcium and magnesium in the test solution were also determined by atomic absorption spectrophotometer.

2.4. Preparation of biomasses

Fungi were grown in potato dextrose broth taken in 250-mL Erlenmeyer flasks. Erlenmeyer flasks containing 75 mL of the medium were incubated at 30 °C for 72 h with shaking (130 rpm) after inoculation with 0.1 mL spore suspension ($\sim$5 × 10^6 spores mL^{-1}). The mycelia were harvested by centrifugation; washed with double distilled water and dried by lyophilization. The dried biomass was used for biosorption studies.

2.5. Adsorption experiment

Each of the adsorbents (0.2 g) was added separately to 50 mL of lead solution (100 mg L^{-1}, pH 3.0, 5.0 and 7.0) taken in different 250-mL Erlenmeyer flasks, and incubated at 30 °C with shaking (130 rpm) for 24 h unless stated otherwise. The flask containing only lead solution (without biomass) serves as control to determine the contribution of the container if any in the adsorption of metal ion. On completion of incubation, the biomass was separated by centrifugation and the concentration of lead in the supernatant was measured. *A. versicolor* biomass (AVB) shows highest adsorption capacity and hence it is selected for further studies. To study the effect of pH and temperature on lead adsorption by AVB, the experiments were conducted over a range of pH 2.0–7.0 and incubation temperature from 20 °C to 40 °C, respectively. The equilibrium adsorption isotherm experiments were executed taking the lead ion concentration range of 25–800 mg L^{-1} at 30 °C and pH 5.0. The adsorption rate of lead by AVB was studied upto 7 h using two different initial metal ion concentrations (100 mg L^{-1} and 200 mg L^{-1}) at 30 °C and pH 5.0. The concentration of lead in the supernatant was determined at regular time intervals. No correction was necessary due to withdrawal of sampling volume since each data point was collected from individual flasks. The concentrations of sodium, potassium, calcium and magnesium in the supernatant after adsorption of lead by AVB at pH 5.0 were also measured vis-à-vis the control flask having only 50 mL distilled water and 0.2 g of biomass. For reusability of the AVB, adsorbed lead was eluted with 0.1 M HCl, washed with double distilled water and again used for the adsorption study.

2.6. Chemical modification of the functional groups of AVB

The functional groups of AVB were modified by chemical treatments as described below. The modified biomass was dried and used for biosorption studies.

2.6.1. Formaldehyde–formic acid
AVB (1 g) was shaken (130 rpm) with a mixture of 20 mL formaldehyde and 40 mL formic acid for 6 h at 30 °C [26].

2.6.2. Triethyl phosphite–nitromethane
AVB (1.0 g) was refluxed with 40 mL of triethyl phosphite and 30 mL nitromethane for 6 h [27].

2.6.3. Acetic anhydride
AVB (1 g) was refluxed with acetic anhydride at 80 °C for 10 h [28].

2.6.4. Methanol–hydrochloric acid
AVB (1 g) was stirred with 70 mL of anhydrous CH$_3$OH and 0.6 mL of concentrated HCl for 6 h at room temperature (30 °C) [29].

2.7. SEM–EDXA study

On completing isotherm experiment with 800 mg L^{-1} of lead and pristine AVB the samples for scanning electron microscopy were prepared as described by Sastri et al. [30]. Micrographs were recorded on FESEM (JEOL JSM – 6700F) equipped with energy dispersive X-ray analyzer.

2.8. FTIR spectroscopy

Fourier transform infrared spectra of pristine and chemically modified AVB were recorded with a Shimadzu FTIR spectrometer (resolution 4 cm^{-1}), equipped with highly sensitive pyroelectric detector (DLATGS). Pressed pellets were prepared by grinding the
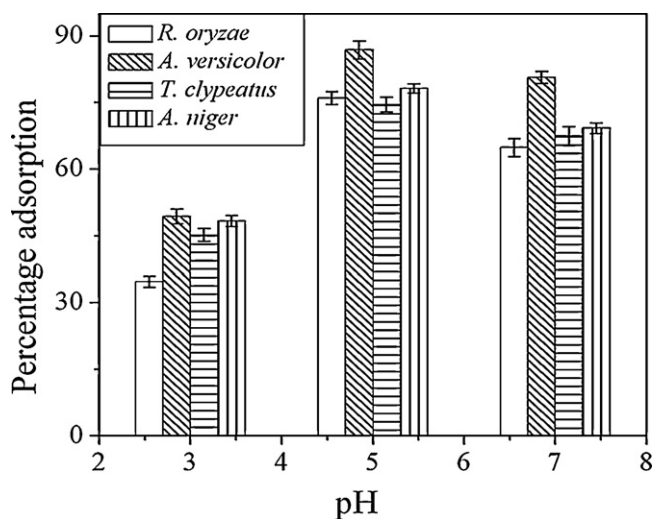
Fig. 1. Adsorption of Pb (II) by different microbial biomasses at 30 °C with initial metal ion concentration of 100 mg L^{-1}. Data represent an average of five independent experiments; ±SD shown by the error bar.

Fig. 2. Effect of pH on Pb (II) adsorption by AVB at 30 °C with initial metal ion concentration of 100 mg L^{-1}. Data represent an average of five independent experiments; ±SD shown by the error bar.

samples with IR grade KBr in an agate mortar with 1:100 ratio and analyzed in the region of 4000–400 cm^{-1}.

2.9. Removal of lead from industrial effluent

The efficiency of AVB to remove lead from an actual system was determined using effluent from battery industries located in Northern region of Kolkata. The removal of lead was carried out as described in Section 2.5 with 50 mL of effluent after adjusting the pH to 5.0.

3. Results and discussion

3.1. Screening of biosorbent

All the four different fungal strains used in the present experiment adsorbed lead from the aqueous solution to the extent of 75–87% depending on the type of the species and pH of the solution (Fig. 1). AVB was found to be the most efficient in this respect over the pH range tested. AVB adsorbed ~87% of lead ions at pH 5.0 under the present experimental conditions. The noted difference in adsorption capacity may be attributed to difference in surface structure and functional groups present on the cell wall of the fungi [31].

3.2. pH and temperature

Adsorption of lead by AVB has been found to increase with increase in pH value to attain maximum at 5.0. It is well known that solution chemistry of the adsorbate depends on the pH of the solution to a great extent and thus influences metal speciation, sequestration or mobility [32–34]. We reported earlier [25] that surface charge of AVB determined from zeta potential measurement varied from +15.1 to −35.5 mV with corresponding changes in pH from pH 2.0 to 8.0 and zero point charge was noted at pH 3.5. Thus it is most likely that at low pH values positively charged surface will not favor the attachment of lead ions due to Columbic repulsion. With increase in pH values, surface becomes more and more negatively charged and thereby favoring lead ion binding. It is observed that adsorption of lead increases with increasing pH values of the solution reaching optimum value at pH 5.0 (Fig. 2). Our findings corroborate the earlier report of Amini et al. [20] on lead adsorption by *A. niger*. It is well established from speciation
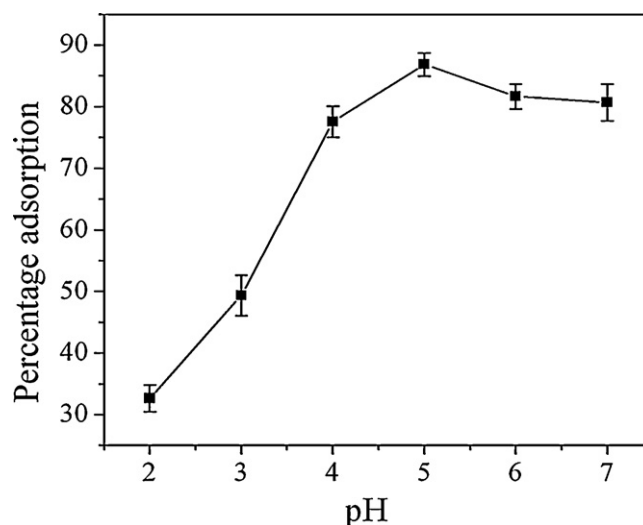
study of single lead species that in an aqueous solution of lead nitrate, the predominant species in the pH range 2.0–6.0 are Pb^{2+}, PbNO$_3^+$ and aqueous Pb(NO$_3$)$_2$. The concentrations of these species do not change until pH 6.0 and the formation of solid Pb(OH)$_2$ starts at pH 6.3 [35]. In aqueous solution metal cations excepting Be^{2+} are generally present in hydrated form and effective sizes of the species are in the order of M^{2+} (aqueous), M(OH)$^{1+}$ (aqueous), M(OH)$_2$ (aqueous) [36]. Thus mobility of the hydrated species having smaller effective size is higher in comparison with larger M^{2+} (aqueous) species and thereby resulting in enhanced adsorption during adsorbate–adsorbent interaction. The noted reduced adsorption at low pH may be attributed to the (i) presence of low mobility higher hydrated species [Pb^{2+} (aqueous)] and (ii) protonation of surface functional groups and competition between H$_3$O$^+$ or H$^+$ and lead ions for the binding sites. At higher pH values (upto 5.0) due to deprotonation more functional groups are exposed for binding with the metal ion leading to higher adsorption. Further increase in pH above 5.0 leads to decrease in adsorption probably due to the formation of soluble hydroxylated complexes of the lead ions and their competition for the active binding sites, as reported earlier in case of cadmium and lead biosorption by mushrooms [37]. No significant change in adsorption of lead ion by the biomass was noted within the investigated temperature range 10–40 °C (Fig. 3). Our findings corroborate the report of Brady and Duncan [38] on copper adsorption by *Saccharomyces cerevisiae*.

3.3. Adsorption isotherm

The efficiency of an adsorbent depends on its capacity to adsorb a particular adsorbate. The adsorption of lead ion on AVB increases with increasing initial metal ion concentration to reach equilibrium at an initial lead ion concentration of 500 mg L^{-1} (Fig. 4A). In order to understand the adsorbate–adsorbent interaction and to design an efficient operating system, it is necessary to analyze the experimental data in the light of different isotherm models, e.g., Langmuir (Eq. (1)), Freundlich (Eq. (2)) and Redlich–Peterson (Eq. (3)) [39–41]:

$$q_e = \frac{a_L K_L C_e}{1 + K_L C_e} \tag{1}$$
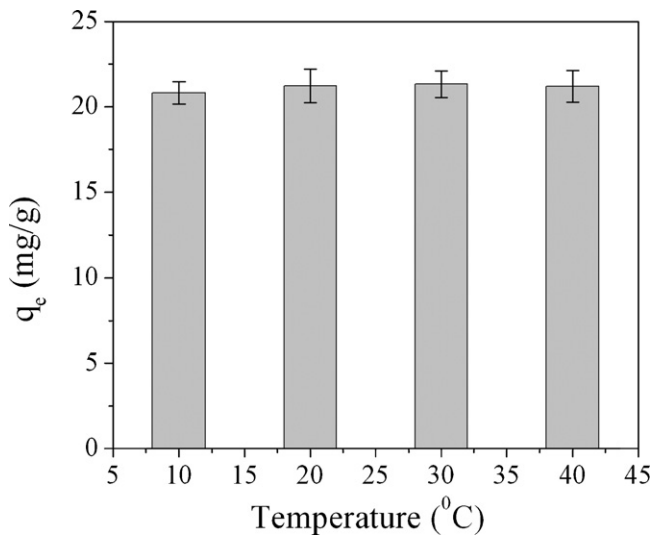
$$q_e = K_F C_e^{1/n} \tag{2}$$

Fig. 3. Effect of incubation temperature on lead adsorption by AVB. Data represent an average of five independent experiments; ±SD shown by the error bar.

where C_e is the equilibrium concentration ($mg\,L^{-1}$) and q_e is the adsorbed amount of metal ion per gram of the biomass at equilibrium ($mg\,g^{-1}$). K_L, a_L and K_F ($L\,g^{-1}$) are the Langmuir and Freundlich constants, respectively, whereas $1/n$ is the heterogeneity factor. The Redlich–Peterson model deals with three parameters:

$$q_e = \frac{AC_e}{1 + BC_e^g} \tag{3}$$

where A ($L\,g^{-1}$) and B ($L\,mg^{-1}$)^g are the Redlich–Peterson constant and 'g' is the Redlich–Peterson isotherm exponent. The value of 'g' lies between 0 and 1, and when $g = 1$, this model converts to the Langmuir model.

All the model parameters are described in Table 1. The "goodness of fit" of the experimental data with the calculated data from the isotherm model can be assessed by R^2 (linear coefficient) and χ^2 (nonlinear coefficient) value. The value of R^2 varies from 0 to 1 and will be very low or zero, if the experimental data differs from the data obtained from the model, whereas the perfect matching of these values yields a coefficient of 1.0. And in case of χ^2, the coefficient value will be small if the experimental data is very close to the obtained data from the model and will higher if they differ. So, it is essential to evaluate the data with both for R^2 and χ^2. The linear regression coefficient (R^2) for Langmuir, Freundlich and Redlich–Peterson model is 0.95, 0.96 and 0.99 and for the nonlinear regression coefficient (χ^2) it is 11.35, 8.09 and 1.98, respectively. Therefore, the present sorption data are found to be best fitted to Redlich–Peterson model (Fig. 4A) in comparison with the other two models considering high correlation coefficient ($R^2 = 0.99$) and low χ^2 value (1.98). This indicates that the adsorption mechanism is a hybrid one and does not follow the ideal monolayer adsorption behavior and this corroborates the earlier report of Pan et al. [42] regarding adsorption of lead by *Bacillus cereus*. The theoretical monolayer saturation capacity (q_{max}), as determined from the Langmuir model ($44.76\,mg\,g^{-1}$) correlates well to the experimentally obtained value ($44.85\,mg\,g^{-1}$). The adsorption capacity of AVB towards lead ($44.85\,mg\,g^{-1}$) is found to be much higher
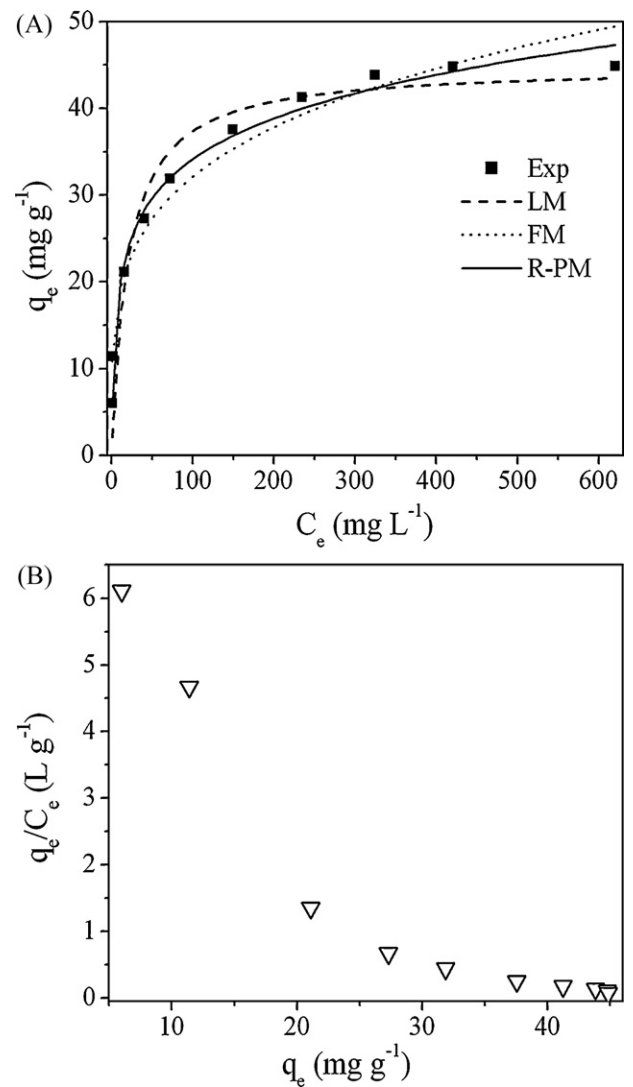

Fig. 4. (A) Equilibrium adsorption isotherm; ■, experimental data; —-, Langmuir model; ·····, Freundlich model; —, Redlich–Peterson model. (B) Scatchard plot analysis of lead adsorption on AVB.

in comparison with most other adsorbents such as *Aspergillus bisporus* ($33.78\,mg\,g^{-1}$), *Phaseolus vulgaris* L. ($42.77\,mg\,g^{-1}$), *Amanita rubescens* ($38.40\,mg\,g^{-1}$) and pretreated *A. versicolor* ($30.6\,mg\,g^{-1}$) as reported earlier by Vimala and Das [37], Özcan et al. [43], Sarı and Tuzen [44] and Çabuk et al. [45], respectively. Surface area as well as surface chemistry of the adsorbent plays important roles in the adsorption of metal ions from its aqueous solution. We reported earlier [25] that BET surface area of AVB is $5.1\,m^2\,g^{-1}$ which is much low compared with other adsorbents [46–48]. Therefore, it may be assumed that besides surface area, other properties such as functional groups present on the biomass play vital roles in the adsorption process by way of interacting with lead ion. Further, lead is a soft acid and biomass being a soft base [49] will prefer to coordinate according to Pearson rule [50]. The sorption data have been further analyzed by Scatchard plot (Eq. (4)) [51] for better

Table 1
Isotherm constants and the values of linear regression coefficient and non linear Chi-square of three isotherm models.

Langmuir				Freundlich				Redlich–Peterson				
R^2	χ^2	q_{max}	K_L	R^2	χ^2	K_F	n	R^2	χ^2	A	B	g
0.95	11.35	44.80	0.05	0.96	8.09	10.81	4.24	0.99	1.98	9.45	0.56	0.83

understanding of the isotherm model:

$$\frac{q}{C} = q_m k_b - q k_b \qquad (4)$$

where q (mg g^{-1}) and C (mg L^{-1}) are the equilibrium adsorption capacity and equilibrium lead ion concentration whereas q_m and k_b are the adsorption isotherm parameters.

Nonlinear Scatchard plot (Fig. 4B) obtained in the present adsorption process suggests that multiple and nonequivalent binding sites are present on the AVB cell surface [51].

3.4. Kinetic study

The rate as well as mechanism of adsorption process can be evaluated from kinetic studies. Significant effect of contact time on the adsorption of lead by AVB is noted which is very fast initially and then gradually slows down to reach equilibrium within 180 min (Fig. 5A). The initial rapid rate is probably due to the presence of abundant active metal binding sites on the biosorbent surface. Subsequently as a result of gradual occupancy of those sites, the rate slows down to reach the equilibrium [52]. The kinetic data are further analyzed by pseudo first (Eq. (5)) (result not shown) and second order (Eq. (6)) [53] model:

$$\ln(q_e - q_t) = \ln q_e - K_L t \qquad (5)$$

$$\frac{t}{q_t} = \frac{1}{K_2 q_e^2} + \frac{t}{q_e} \qquad (6)$$

where q_e (mg g^{-1}) and q_t (mg g^{-1}) are the amounts of lead adsorbed at equilibrium and time 't', respectively. K_L and K_2 are the rate constants of pseudo first and second order rate equations, respectively.

The experimental data (Fig. 5B) indicate that the adsorption kinetics follow pseudo second order rate equation ($R^2 = 0.999$) and chemisorption is the rate limiting step for the removal of lead by AVB under the studied experimental conditions [44]. The kinetic rate models could not establish the diffusion mechanism so; sorption kinetic data was further analyzed to understand the role of intraparticle diffusion in the present adsorption process. Intraparticle diffusion model (Eq. (7)) [54] can be characterized by the relationship between specific sorption capacity at time 't' and the square root of the time:

$$q_t = K_p t^{1/2} + C \qquad (7)$$

where q_t (mg g^{-1}) is the amounts of lead adsorbed at time 't'. K_p is the intraparticle diffusion rate constant (mg g^{-1} min$^{-1/2}$) and C is the intercept (mg g^{-1}). The nonlinear nature of the curve and deviation of plots from the origin (Fig. 5C) indicates that the intraprticle diffusion is not the rate limiting step for the whole adsorption process [55].

3.5. Binding mechanism

Scanning electron microscopy is used to characterize the surface morphology of a biosorbent [56] which shows that the, surface morphology of the pristine AVB (Fig. 6A) is conspicuously different from that of the lead adsorbed species (Fig. 6B). The smooth flakes like surface of the pristine mycelia, turned rough and irregular after the adsorption of lead ion. Highly magnified image (Fig. 6C) of the post adsorbed AVB (marked area) demonstrates the presence of lead nanoparticulates on the mycelial surface. The EDXA spectra show the presence of lead in place of sodium, potassium, calcium and magnesium indicating the adsorption of lead
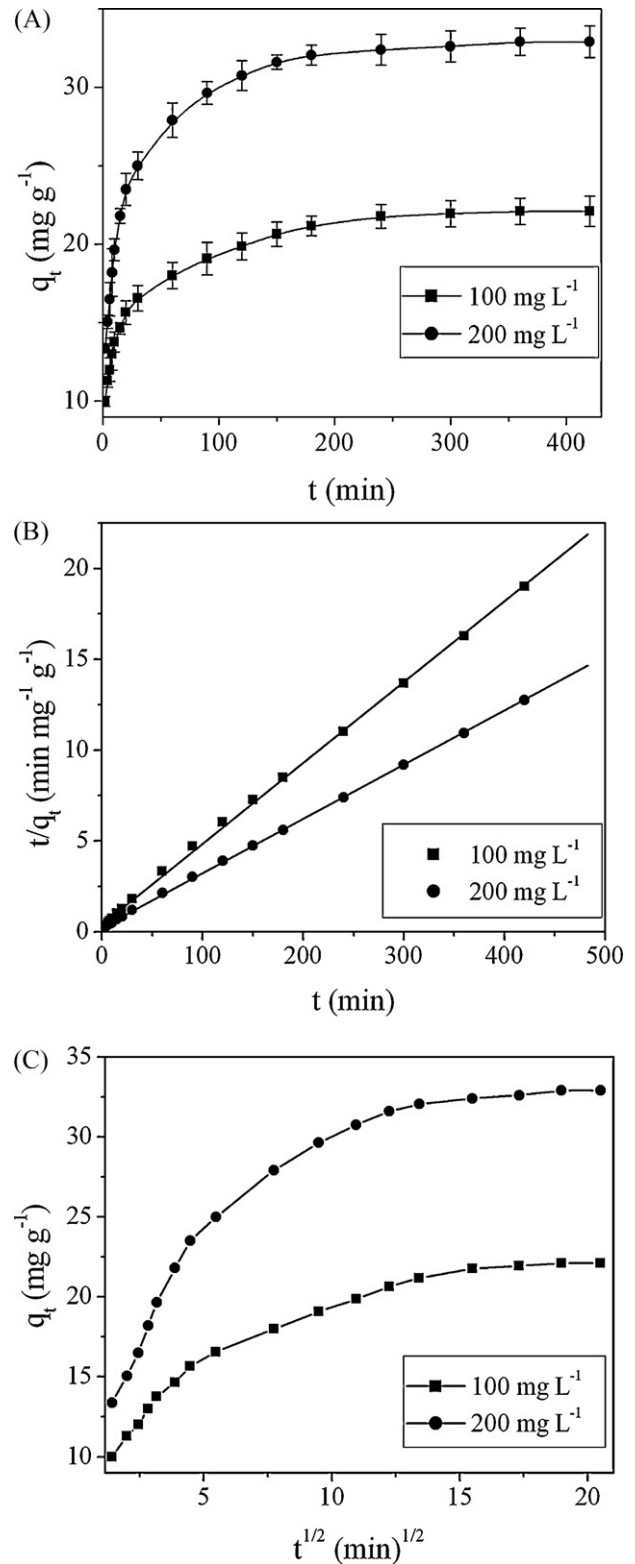

Fig. 5. The effect of contact time (A) and pseudo second order plot (B) of lead removal on AVB at different initial metal ion concentration. Intraparticular diffusion on lead binding by AVB (C). Data represent an average of five independent experiments; ±SD shown by the error bar.

on AVB occurs through ion exchange mechanism (Fig. 6D and E). To further validate the ion exchange mechanism during lead adsorption, the concentrations of different cations (Na$^+$, K$^+$, Ca^{2+} and Mg^{2+}) in the test solution were also measured. The results obtained demonstrate that potassium, calcium and sodium ions
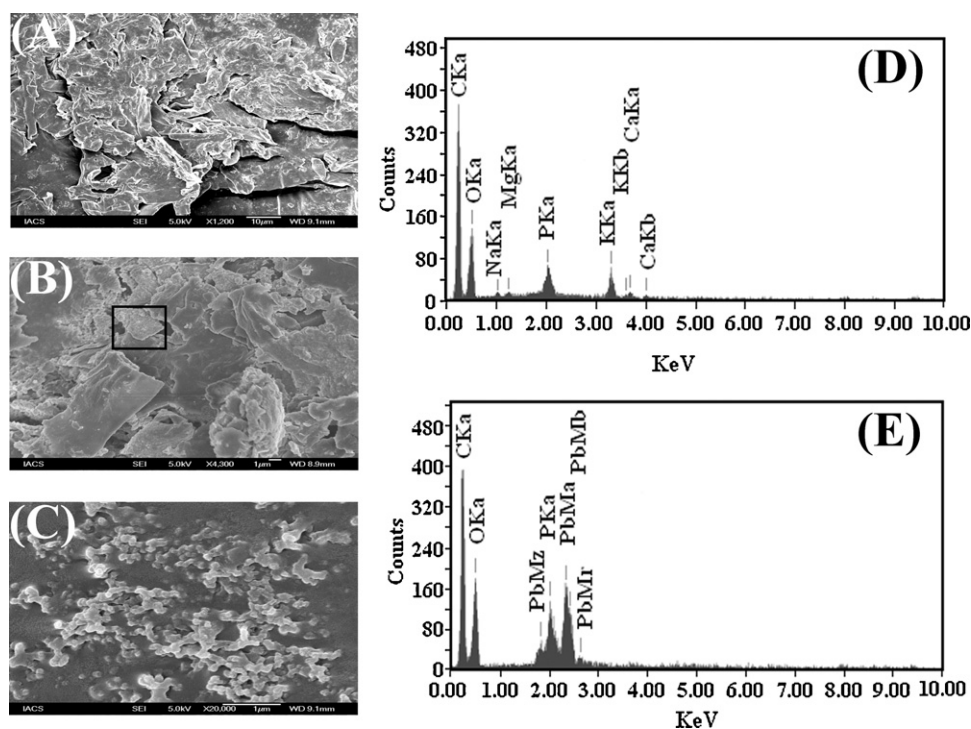
Fig. 6. Scanning electron micrograph of *A. versicolor* biomass. (A) Pristine biomass; (B) lead adsorbed biomass and (C) lead loaded AVB at higher magnification. EDX spectra of pristine AVB (D) and lead loaded AVB (E).

Table 2
Release of Na$^+$, K$^+$, Ca^{2+} and Mg^{2+} due to adsorption of Pb (II) on *Aspergillus versicolor* biomass.

Total Pb^{+2} adsorbed (mequiv. g^{-1})	Net amount of cation released (mequiv. g^{-1})[a]				Total amount of cations released (mequiv. g^{-1})	Bound lead/cations released ($R_{b/r}$)[b]
	K$^+$	Na$^+$	Ca^{2+}	Mg^{2+}		
1.041	0.288	0.221	0.203	0.025	0.738	1.41

Initial lead ion concentration: 100 mg L^{-1}.

[a] Difference between metal released after adsorption and that by the control.

[b] $R_{b/r}$: ratio of metal bounded to cations released.

take part in the ion exchange process. The amount of magnesium released has less impact on ion exchange phenomenon compared with other cations (Table 2). The ratio of bound to released metal cations (>1) shows that other mechanisms are also involved in the lead biosorption process. The role of ion exchange mechanism in the adsorption of lead by microbial biomass and agro waste materials was also reported by other workers [31,57–59]. The proposed mechanism for lead adsorption on AVB is represented schematically in Fig. 7.

Fourier transform infrared spectroscopy can be employed to identify the functional groups present on the cell surface of AVB because, each group has a unique energy absorption band. FTIR spectrum of pristine AVB (Fig. 8A) exhibits distinct peaks suggesting the presence of amine, carboxyl, phosphate and hydroxyl groups. The broad mixed stretching vibrations frequency of N–H and O–H are observed in the region of 3500–3300 cm^{-1} and those for alkyl chains around 2920–2850 cm^{-1}. The sharp peak at 1652.88 cm^{-1} can be attributed to C=O stretching of carboxyl or amide groups. The band at 1550.66 cm^{-1} is assigned to N–H bending. The presence of COO$^-$ of the carboxylate can be attributed to the peak positions at 1452.30 cm^{-1} and 1400.22 cm^{-1} on the biomass. The complex amide III band is located near 1319.22 cm^{-1}. The wave number at 1026.06 cm^{-1} arises due to the presence of P–O–C link of the organo

phosphorous groups on the biomass. The shift of around 4 cm^{-1} in the FTIR analysis may be due to the resolution of the device. In the present case the shift of more than 4 cm^{-1} was only considered. FTIR spectrum of AVB after lead adsorption (Fig. 8B) depicts that the peak at 1550.66 cm^{-1} assigned to N–H bending shifts to 1552.59 cm^{-1} indicating that the nitrogen atom is not the main adsorption site for lead attachment on AVB. A small shift in the wave number from 2929.67 cm^{-1} to 2925.81 cm^{-1} is noted after lead adsorption and this may be due to change in C–H vibration for adsorption. The observed result may be due to oxygen atom in the hydroxyl group, which could be involved in lead adsorption. However, the spectral shift is very close to 4 cm^{-1} and it may be inferred that the hydroxyl group is not the responsible site for lead adsorption. The changes in transmittance along with the spectral shift at the wave number 1652.88 cm^{-1} suggest the involvement of C=O of carboxyl or amide group. The disappearance of band at 1452.30 cm^{-1} and 1400.22 cm^{-1} and formation of a new band at 1382.87 cm^{-1} suggest the involvement of COO$^-$ of the carboxylate group. The characteristic changes in transmittance in the region 1026.06–1035.70 cm^{-1} during lead adsorption on AVB, may result due to phosphorous interference.

Adsorption of metal ions mainly involves the functional groups present on the microbial cell surface [60]. The functional groups
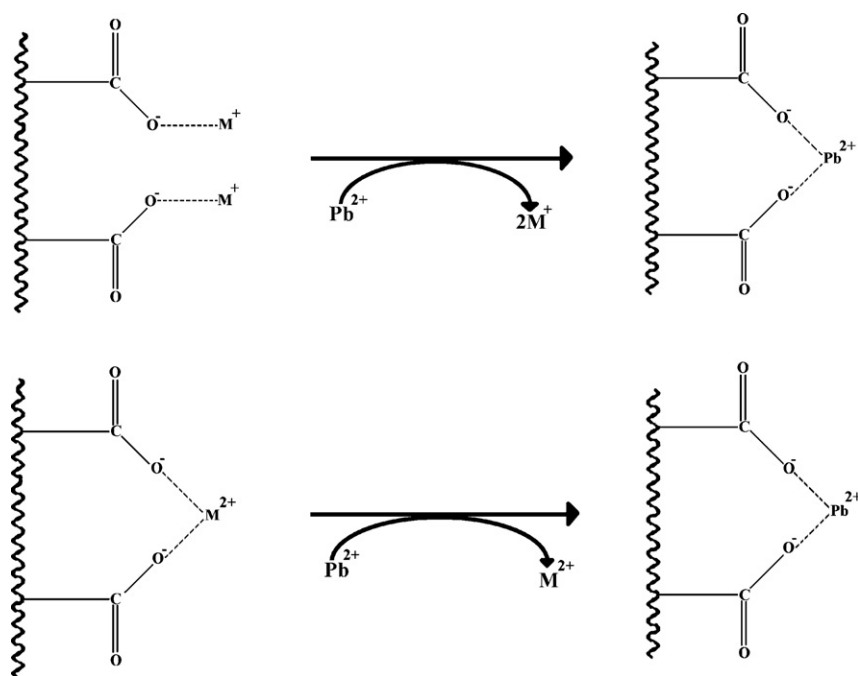
Fig. 7. Proposed cation exchange mechanism for lead removal by AVB. M^+ and M^{2+} represents monovalent (Na^+ and K^+) and divalent (Ca^{2+} and Mg^{2+}) cations. respectively.

such as carboxyl, phosphate, amino and hydroxyl groups of AVB were chemically modified to understand their role in lead adsorption process. Formaldehyde and formic acid methylates the primary and secondary amines present on the cell surface of AVB according to the reaction scheme shown below:

$$R–NH_2 + 2HCHO + 2HCOOH \rightarrow R–N(CH_3)_2 + 2CO_2 + 2H_2O$$
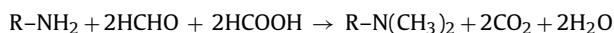
The methylation of amino group does not alter the adsorption capacity of lead suggesting insignificant role of the amino groups in the adsorption of lead on AVB.

Refluxing with acetic anhydride causes the acetylation of the hydroxyl group present on AVB. The general reaction scheme is:

$$R–CH_2OH + (CH_3CO)_2 \rightarrow R–CH_2COCH_3 + CH_3COOH$$
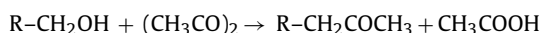
Since no change in adsorption of lead is noted due to blocking of hydroxyl groups of AVB, it is likely that this group is not involved in the adsorption process.

Treatment of AVB with anhydrous methanol and HCl results in the esterification of the carboxyl group. The general reaction scheme is shown below:

$$R–COOH + CH_3OH \rightarrow R–COOCH_3 + H_2O$$
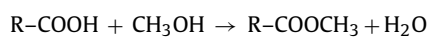
Esterification of the carboxyl group reduced the adsorption capacity by 57.16%, indicating that the carboxyl groups present on AVB play a crucial role in lead adsorption.

AVB on refluxing with triethyl phosphite and nitromethane blocks the phosphate group of orthophosphoric acid present on the AVB cell surface. The reduction of lead adsorption capacity by 15.65% suggests the involvement of phosphate group on the process.

The experimental findings are also supported by the non linear nature of the Schatchard plot which suggests the presence of multiple lead adsorption sites on AVB.
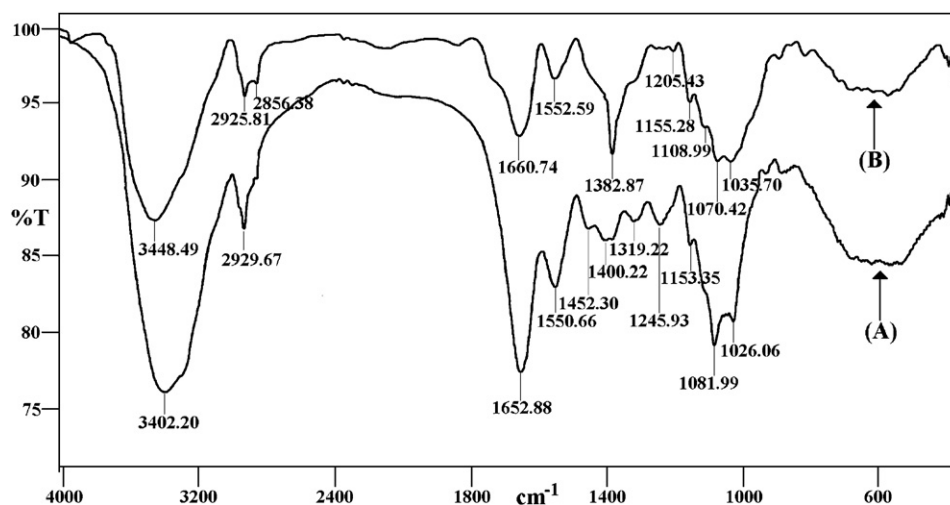

Fig. 8. FTIR spectra of pristine (A) and lead adsorbed AVB (B).

Table 3
Removal of Pb (II) from industrial effluent by AVB.

Concentration of Pb (II) in industrial effluent before treatment (mg L^{-1})	Concentration of Pb (II) in industrial effluent after treatment (mg L^{-1})
3.20	0.45
5.10	0.72

3.6. Reusability of AVB

Desorption of lead from the lead adsorbed biomass to the extent of 85% can be achieved with 0.1 M HCl and the biomass can again be used for adsorption of lead. The adsorption–desorption cycle can be conducted for five times after which loss in activity was noted probably due to loss of integrity of the cell (data not shown). Thus we believe that adsorption involving AVB is a highly effective and efficient methodology for removing lead from polluted waterbodies.

3.7. Interaction of lead with AVB in industrial effluent

The efficiency of AVB to remove lead was also executed using the effluent of battery industry as a feed solution. The concentration of lead in the effluent varied from 3.2 mg L^{-1} to 5.1 mg L^{-1}. The adsorption experiment was carried out after adjusting the pH at 5.0. It was observed that the percentage removal of lead from industrial effluent was 86% (Table 3). This value is very similar to that obtained from the monometallic system, suggesting that the presence of anions and cations present in the industrial effluent has no inhibitory effect on lead adsorption under the studied experimental condition.

4. Conclusion

We demonstrate a viable option for the removal of lead from contaminated water with AVB. The maximum adsorption capacity of AVB has been found to be 45 mg Pb (II) per gram of the dry weight of the biomass. The Redlich–Peterson isotherm model describes the adsorption process satisfactorily suggesting that the adsorption mechanism is a hybrid one and does not follow ideal monolayer adsorption and the possibility of multilayer adsorption. Scatchard plot analysis reveals multiple and non equivalent binding sites on the AVB cell surface. The adsorption process is very fast initially and more than 80% is completed within 60 min. FTIR study and chemical modifications of biomass cell surface suggest the major involvement of carboxyl functional groups in the adsorption process. Thus it may be summarized that AVB can remove lead from its aqueous solution successfully.

Acknowledgements

References

[1] M. Nadeem, A. Mahmood, S.A. Shahid, S.S. Shah, A.M. Khalid, G. Mckay, Sorption of lead from aqueous solution by chemically modified carbon adsorbents, J. Hazard. Mater. B 138 (2006) 604–613.

[2] V.K. Gupta, A. Rastogi, Biosorption of lead from aqueous solutions by green algae *Spirogyra* species: kinetics and equilibrium studies, J. Hazard. Mater. 152 (2008) 407–414.

[3] C. Raji, T.S. Anirudhan, Chromium (VI) adsorption by sawdust carbon: kinetics and equilibrium, Indian J. Chem. Technol. 4 (1997) 228–236.

[4] A. Ornek, M. Ozacar, I.A. Sengil, Adsorption of lead onto formaldehyde or sulphuric acid treated acorn waste: equilibrium and kinetic studies, Biochem. Eng. J. 37 (2007) 192–200.

[5] K. Jayaram, I.Y.L.N. Murthy, H. Lalhruaitluanga, M.N.V. Prasad, Biosorption of lead from aqueous solution by seed powder of *Strychnos potatorum* L., Colloids Surf. B: Biointerfaces 71 (2009) 248–254.

[6] W.Y. Baik, J.H. Bae, K.M. Cho, W. Hartmeier, Biosorption of heavy metals using whole mold mycelia and parts thereof, Bioresour. Technol. 81 (2002) 167–170.

[7] A. Demirbas, Heavy metal adsorption onto agro-based waste materials: a review, J. Hazard. Mater. 157 (2008) 220–229.

[8] J. Cruz-Olivares, C. Pérez-Alonso, C. Barrera-Díaz, G. López, P. Balderas-ernández, Inside the removal of lead(II) from aqueous solutions by de-oiled allspice husk in batch and continuous processes, J. Hazard. Mater. 181 (2010) 1095–1101.

[9] F. Veglio, F. Beolchini, Removal of metals by biosorption: a review, Hydrometallurgy 44 (1997) 301–316.

[10] J.M.C. Tobin, C. White, G.M. Gadd, Metal accumulation by fungi: applications in environmental biotechnology, J. Ind. Microbiol. Biotechnol. 13 (1994) 126–130.

[11] P.G.G. Burnett, C.J. Daughney, D. Peak, Cd adsorption onto *Anoxybacillus flavithermus*: surface complexation modeling and spectroscopic investigations, Geochim. Cosmochim. Acta 70 (2006) 5253–5269.

[12] J.B. Fein, D.A. Fowle, J. Cahill, K. Kemner, M. Boyanov, B. Bunker, Nonmetabolic reduction of Cr(VI) by bacterial surfaces under nutrient-absent conditions, Geomicrobiol. J. 19 (2002) 369–382.

[13] A.Y. Dursun, A comparative study on determination of the equilibrium, kinetic and thermodynamic parameters of biosorption of copper (II) and lead (II) ions onto pretreated *Aspergillus niger*, Biochem. Eng. J. 28 (2006) 187–195.

[14] B. Volesky, Biosorption and me, Water Res. 41 (2007) 4017–4029.

[15] J.N.L. Latha, K. Rashmi, M.P. Maruthi, Cell-wall-bound metal ions are not taken up in *Neurospora crassa*, Can. J. Microbiol. 51 (2005) 1021–1026.

[16] J. Wang, C. Chen, Biosorption of heavy metals by *Saccharomyces cerevisiae*: a review, Biotechnol. Adv. 24 (2006) 427–451.

[17] Y.S. Saˇg, T. Kutsal, Determination of the biosorption heats of heavy metal ions on *Zoogloea ramigera* and *Rhizopus arrhizus*, Biochem. Eng. J. 6 (2000) 145–151.

[18] T. Fan, Y. Liu, B. Feng, G. Zeng, C. Yang, M. Zhou, H. Zhou, Z. Tan, X. Wang, Biosorption of cadmium(II), zinc(II) and lead(II) by *Penicillium simplicissimum*: isotherms, kinetics and thermodynamics, J. Hazard. Mater. 160 (2008) 655–661.

[19] W. Jianlong, Z. Xinmin, D. Decai, Z. Ding, Biosorption of lead (II) from aqueous solution by fungal biomass of *Aspergillus niger*, J. Biotechnol. 87 (2001) 273–277.

[20] M. Amini, H. Younesi, N. Bahramifar, A.A.Z. Lorestani, F. Ghorbani, A. Daneshi, M. Sharifzadeh, Application of response surface methodology for optimization of lead biosorption in an aqueous solution by *Aspergillus niger*, J. Hazard. Mater. 154 (2008) 694–702.

[21] A. Kapoor, T. Viraraghavan, D.R. Cullimore, Removal of heavy metals using the fungus *Aspergillus niger*, Bioresour. Technol. 70 (1999) 95–104.

[22] S.K. Das, A.K. Guha, Biosorption of chromium by *Termitomyces clypeatus*, Colloids Surf. B: Biointerfaces 60 (2007) 46–54.

[23] S.K. Das, A.K. Guha, Biosorption of hexavalent chromium by *Termitomyces clypeatus* biomass: kinetics and transmission electron microscopic study, J. Hazard. Mater. 167 (2009) 685–691.

[24] S. Majumdar, S.K. Das, T. Saha, G.C. Panda, T. Bandyopadhyou, A.K. Guha, Adsorption behavior of copper ions on *Mucor rouxii* biomass through microscopic and FTIR analysis, Colloids Surf. B: Biointerfaces 63 (2008) 138–145.

[25] S.K. Das, A.R. Das, A.K. Guha, A study on the adsorption mechanism of mercury on *Aspergillus versicolor* biomass, Environ. Sci. Technol. 41 (2007) 8281–8287.

[26] G.M. Loudon, Organic Chemistry, First ed., Reading, MA, USA, Addison-Wesley, 1984.

[27] A. Markowska, J. Olejnik, J. Michalski, Selektive Alkylierung von mehrbasigen Sa¨uren des 4-bindigen Phosphors mit Trialkylphosphit, Chem. Ber. 108 (1975) 2589–2592.

[28] L.F. Fieser, M. Fieser, Reagents for Organic Synthesis, vol. 1, Wiley, New York, 1967.

[29] J. Gardea-Torresdey, M.K. Becker-Hapak, J.M. Hosea, D.W. Darnall, Effect of chemical modification of algal carboxyl groups on metal ion binding, Environ. Sci. Technol. 24 (1990) 1372–1378.

[30] M. Sastri, A. Ahmad, M.I. Khan, R. Kumar, Biosynthesis of metal nanoparticles using fungi and actinomycete, Curr. Sci. 85 (2003) 162–170.

[31] W. Lo, H. Chua, K.-H. Lam, S.-P. Bi, A comparative investigation on the biosorption of lead by filamentous fungal biomass, Chemosphere 39 (1999) 2723–2736.

[32] J.D. Merifield, W.G. Davids, J.D. MacRae, A. Amirbahman, Uptake of mercury by thiol-grafted chitosan gel beads, Water Res. 38 (2004) 3132–3138.

[33] P. Miretzky, M.C.B.M.F. Jardim, J.C. Rocha, Factors affecting Hg(II) adsorption in soils from the Rio Negro Basin (Amazon), Quim. Novo 28 (2005) 438–443.

[34] S. Kraemer, J.G. Hering, Biogeochemical controls on the mobility and bioavailability of metals in soils and groundwater, Aquat. Sci. 66 (2004) 1–2.

[35] G. Issabayeva, M.K. Aroua, N.M.N. Sulaiman, Removal of lead from aqueous solutions on palm shell activated carbon, Bioresour. Technol. 97 (2006) 2350–2355.

[36] B. Xiao, K.M. Thomas, Adsorption of aqueous metal ions on oxygen and nitrogen functionalized nanoporous activated carbons, Langmuir 21 (2005) 3892–3902.

[37] R. Vimala, N. Das, Biosorption of cadmium (II) and lead (II) from aqueous solutions using mushrooms: a comparative study, J. Hazard. Mater. 168 (2009) 376–382.

[38] D. Brady, J.R. Duncan, Bioaccumulation of metal cations by *Saccharomyces cerevisiae*, Appl. Microbiol. Biotechnol. 41 (1994) 149–154.

[39] I. Langmuir, The adsorption of gases on plane surfaces of glass, mica and platinum, J. Am. Chem. Soc. 40 (1918) 1361–1403.

[40] H.M.F. Freundlich, Über die adsorption in lösungen, Z. Phys. Chem. (Leipzig) 57A (1906) 385–470.

[41] O. Redlich, D.L. Peterson, A useful adsorption isotherm, J. Phys. Chem. 63 (1959) 1024–1026.

[42] J. Pan, X. Ge, R. Liu, H. Tang, Characteristic features of *Bacillus cereus* cell surfaces with biosorption of Pb (II) ions by AFM and FT-IR, Colloids Surf. B: Biointerfaces 52 (2006) 89–95.

[43] A.S. Özcan, S. Tunali, T. Akar, A. Özcan, Biosorption of lead (II) ions onto waste biomass of *Phaseolus vulgaris L.*: estimation of the equilibrium, kinetic and thermodynamic parameters, Desalination 244 (2009) 188–198.

[44] A Sarı, M. Tuzen, Kinetic and equilibrium studies of biosorption of Pb (II) and Cd (II) from aqueous solution by macrofungus (*Amanita rubescens*) biomass, J. Hazard. Mater. 164 (2009) 1004–1011.

[45] A. Çabuk, S. Ilhan, C. Filik, F. Caliskan, Pb^{2+} biosorption by pretreated fungal biomass, Turk. J. Biol. 29 (2005) 23–28.

[46] J. Goel, K. Kadirvelu, C. Rajagopal, V.K. Garg, Removal of mercury (II) from aqueous solution by adsorption on carbon earogel: response surface methodological approach, Carbon 43 (2005) 197–200.

[47] F.-S. Zhang, J.O. Nriagu, H. Itoh, Mercury removal from water using activated carbons derived from organic sewage, Water Res. 39 (2005) 389–395.

[48] B. Tansel, P. Nagarajan, SEM study of phenolphthalein adsorption on granular activated carbon, Adv. Environ. Res. 8 (2004) 411–415.

[49] S.V. Avery, J.M. Tobin, Mechanism of adsorption of hard and soft metal ions to *Saccharomyces cerevisiae* and influence of hard and soft anions, Appl. Environ. Microbiol. 59 (1993) 2851–2856.

[50] R.G. Pearson, Absolute electronegativity and hardness: application, Inorg. Chem. 27 (1988) 734–740.

[51] J.M. Tobin, D.G. Copper, R.J. Neufeld, Investigation of the mechanism of metal uptake by denatured *Rhizopus arrhizus* biomass, Enzyme Microb. Technol. 12 (1990) 591–595.

[52] J.P. Chen, L. Wang, Characterization of metal adsorption kinetic properties in batch and fixed-bed reactors, Chemosphere 54 (2004) 397–404.

[53] S.T. Akar, A. Gorgulu, Z. Kaynak, B. Anilan, T. Akar, Biosorption of reactive blue 49 dye under batch and continuous mode using a mixed biosorbent of macrofungus *Agaricus bisporus* and *Thuja orientalis* cones, Chem. Eng. J. 148 (2009) 26–34.

[54] F. Çolak, N. Atar, A. Olgun, Biosorption of acidic dyes from aqueous solution by *Paenibacillus macerans*: kinetic, thermodynamic and equilibrium studies, Chem. Eng. J. 150 (2009) 122–130.

[55] M.N. Sahmoune, K. Louhab, A. Boukhiar, Kinetic and equilibrium models for the biosorption of Cr (III) on *Streptomyces rimosus*, Res. J. Appl. Sci. 3 (4) (2008) 294–301.

[56] L. Mogollon, R. Rodriguez, W. Larrota, N. Ramirez, R. Torres, Biosorption of nickel using filamentous fungi, Appl. Biochem. Biotechnol. 70–72 (1998) 593–601.

[57] T. Akar, S. Tunali, A. Çabuk, Study on the characterization of lead (II) biosorption by fungus *Aspergillus parasiticus*, Appl. Biochem. Biotechnol. 136 (2007) 389–405.

[58] M. Iqbal, A. Saeed, S.I. Zafar, FTIR spectrophotometry, kinetics and adsorption isotherms modeling, ion exchange, and EDX analysis for understanding the mechanism of Cd^{2+} and Pb^{2+} removal by mango peel waste, J. Hazard. Mater. 164 (2009) 161–171.

[59] M. Martinez, N. Miralles, S. Hidalgo, N. Fiol, I. Villaescusa, J. Poch, Removal of lead (II) and cadmium (II) from aqueous solutions using grape stalk waste, J. Hazard. Mater. B 133 (2006) 203–211.

[60] J.B. Fein, C.J. Daughney, N. Yee, T.A. Davis, A chemical equilibrium model for metal adsorption onto bacterial surfaces, Geochim. Cosmochim. Acta 61 (1997) 3319–3328.